

Simulation of
atmospheric mercury
depletion events

Z.-Q. Xie et al.

Simulation of atmospheric mercury depletion events (AMDEs) during polar springtime using the MECCA box model

Z.-Q. Xie^{1,*}, R. Sander², U. Pöschl¹, and F. Slemr²

¹Biogeochemistry Department, Max Planck Institute for Chemistry, P.O. Box 3060,
55020 Mainz, Germany

²Air Chemistry Department, Max Planck Institute for Chemistry, P.O. Box 3060,
55020 Mainz, Germany

*also at: Institute of Polar Environment, University of Science and Technology of China, Hefei,
Anhui, 230026, The P R China

Received: 7 May 2008 – Accepted: 12 June 2008 – Published: 10 July 2008

Correspondence to: Z.-Q. Xie (zqxie@mpchmainz.mpg.de)

Published by Copernicus Publications on behalf of the European Geosciences Union.

Title Page

Abstract

Introduction

Conclusions

References

Tables

Figures

◀

▶

◀

▶

Back

Close

Full Screen / Esc

Printer-friendly Version

Interactive Discussion



Abstract

Atmospheric mercury depletion events (AMDEs) during polar springtime are closely correlated with bromine-catalyzed tropospheric ozone depletion events (ODEs). To study gas- and aqueous-phase reaction kinetics and speciation of mercury during AMDEs, we have included mercury chemistry into the box model MECCA (Module Efficiently Calculating the Chemistry of the Atmosphere), which enables dynamic simulation of bromine activation and ODEs.

We found that the reaction of Hg with Br atoms dominates the loss of gaseous elemental mercury (GEM). To explain the experimentally observed synchronous destruction of Hg and O₃, the reaction rate of Hg+BrO has to be much lower than that of Hg+Br. The synchronicity is best reproduced with rate coefficients at the lower limit of the literature values for both reactions, i.e. $k_{\text{Hg}+\text{Br}} \approx 3 \times 10^{-13}$ and $k_{\text{Hg}+\text{BrO}} \leq 1 \times 10^{-15} \text{ cm}^3 \text{ mol}^{-1} \text{ s}^{-1}$, respectively.

Throughout the simulated AMDEs, BrHgOBr was the most abundant reactive mercury species, both in the gas phase and in the aqueous phase. The aqueous phase concentrations of BrHgOBr, HgBr₂, and HgCl₂ were several orders of magnitude larger than that of Hg(SO₃)₂²⁻.

Considering chlorine chemistry outside depletion events (i.e. without bromine activation), the concentration of total divalent mercury in sea-salt aerosol particles (mostly HgCl₂) was much higher than in dilute aqueous droplets (mostly Hg(SO₃)₂²⁻), and did not exhibit a diurnal cycle (no correlation with HO₂ radicals).

1 Introduction

Mercury is a prominent environmental pollutant which can form toxic compounds and bioaccumulate in aquatic organisms and food chains. Due to its relatively high vapor pressure and low solubility, mercury undergoes long-range atmospheric transport to remote areas like the polar regions.

ACPD

8, 13197–13233, 2008

Simulation of atmospheric mercury depletion events

Z.-Q. Xie et al.

Title Page

Abstract

Introduction

Conclusions

References

Tables

Figures

⏪

⏩

◀

▶

Back

Close

Full Screen / Esc

Printer-friendly Version

Interactive Discussion



**Simulation of
atmospheric mercury
depletion events**

Z.-Q. Xie et al.

Title Page

Abstract

Introduction

Conclusions

References

Tables

Figures

◀

▶

◀

▶

Back

Close

Full Screen / Esc

Printer-friendly Version

Interactive Discussion

Since 1995, year-round monitoring of atmospheric Hg has been performed at Alert, Canada (Schroeder et al., 1998). The results indicate that gaseous elemental mercury (GEM, Hg⁰) concentrations occasionally decrease from approximately 1.7 ng/m³, the background level in the Northern Hemisphere (Slemr et al., 2003), to values less than 0.1 ng/m³ within 24 h or less after sunrise from late March to mid-June. Such abrupt losses of GEM are called atmospheric mercury depletion events (AMDEs), and they are closely correlated with ground level ozone depletion events (ODEs). Further investigations at Barrow, Ny-Ålesund, and Station Nord (northeast Greenland) showed that AMDEs can occur throughout the Arctic and the sub-Arctic regions (Lindberg et al., 2002; Berg et al., 2003; Skov et al., 2004; Poissant and Pilote, 2003). Highly time-resolved measurements of mercury species and total gaseous mercury (TGM) at the Neumayer station (Ebinghaus et al., 2002; Temme et al., 2003) and at Terra Nova Bay (Sprovieri et al., 2002) revealed that AMDEs occur also in the maritime Antarctic during austral spring. The chemical processes involved in AMDEs are, however, still not well understood, as outlined in a recent review by Steffen et al. (2008).

The depletion of GEM is thought to be due to conversion into reactive gas-phase mercury (RGM) and into particulate mercury. Lu et al. (2001) and Lu and Schroeder (2004) found an anti-correlation between measured GEM and the concentration of particulate mercury during AMDEs at Alert in 1998. The chemical reactions causing the AMDEs (Lindberg et al., 2001; Ariya et al., 2002; Lindberg et al., 2002; Calvert and Lindberg, 2004b; Goodsite et al., 2004) are probably similar to those driving the ozone depletion events (Bottenheim et al., 1986; Barrie et al., 1988; Simpson et al., 2007), and the oxidation of GEM by reactive halogen species like Br atoms and BrO radicals is considered to be a key process of mercury depletion (Ariya et al., 2004; Calvert and Lindberg, 2004a; Goodsite et al., 2004; Skov et al., 2004).

Reactive bromine species can be generated from sea salt aerosols and in the course of sea ice formation, when concentrated salt solutions (brine) are separated from ice. When an open lead of sea water begins to freeze over, it often forms frost flowers. These are dendritic vapor-deposited ice crystals that wick brine from the freezing ice

(Perovich and Richter-Menge, 1994; Rankin et al., 2002; Canosa-Mas et al., 1996) and can serve as sites of halogen activation and sources of sea salt aerosols (Simpson et al., 2007). Recently, Sander et al. (2006) used the MECCA box model to study the role of carbonate precipitation in freezing sea water for the generation of reactive bromine. To link the process of halogen activation in sea salt aerosols over nascent sea ice with AMDEs and investigate its potential impact, we have added mercury chemistry to MECCA.

For comparison, other model studies of atmospheric mercury chemistry are listed in Table 1 and shortly summarized here. Ryaboshapko et al. (2002) compared several mercury chemistry models. These models have been commonly used to study the long-range transport of mercury. They contain chemical reactions of Hg species related to SO₂ and chlorine but they do not consider bromine chemistry. Pan and Carmichael (2005) studied mercury atmospheric mechanisms with a box model, assuming gas/aqueous-phase partitioning according to Henry's law. Outside of the polar regions, only a few studies include bromine chemistry. Hedgecock et al. (2005) added bromine chemistry to AMCOTS (Atmospheric Mercury Chemistry Over the Sea) and studied the Mediterranean marine boundary layer. Shon et al. (2005) modeled atmospheric mercury and bromine chemistry in urban air in a coastal city. Within the Arctic region, two hemispheric models (DEHM by Christensen et al. (2004) and MSCE-Hg by Travnikov (2005)) and a global model (GRAHM by Dastoor and Larocque (2004)) have been used to model AMDEs. The mercury chemistry in these studies is mostly based on the scheme from Petersen et al. (1998), which does not include bromine chemistry. Skov et al. (2004) developed a parameterization for DEHM to study AMDEs. However, they could not describe the fast variations of GEM as observed during spring. Calvert and Lindberg (2003) studied the influence of bromine chemistry on AMDEs. Their simulated rate of Hg depletion is dependent on the Hg+BrO reaction. Since the concentration of the BrO radical will be many times that of the Br atoms in the O₃-rich troposphere, BrO may thus be an important oxidant for GEM. However, their model used prescribed fluxes of Br₂ and BrCl, and the mechanism did not consider aqueous-

Simulation of atmospheric mercury depletion events

Z.-Q. Xie et al.

Title Page

Abstract

Introduction

Conclusions

References

Tables

Figures

◀

▶

◀

▶

Back

Close

Full Screen / Esc

Printer-friendly Version

Interactive Discussion



phase reactions. To the best of our knowledge, the work presented here is the first model study of AMDEs including bromine chemistry with a fully coupled gas/aqueous chemistry mechanism.

2 Model description

We have used the atmospheric chemistry box model MECCA (Module Efficiently Calculating the Chemistry of the Atmosphere) by [Sander et al. \(2005\)](#). Recently, it has been applied to investigate the role of carbonate precipitation in ODEs ([Sander et al., 2006](#)). It describes the release of halogens from sea salt aerosols under conditions of the polar boundary layer at 82° N with a fully pH-dependent aqueous-phase chemistry mechanism. Here, we added mercury chemistry to the polar MECCA model. In the current model version, there are a total of 686 equations (178 gas phase equations, 250 aqueous phase equations, 138 Henry's law equations, 70 equilibria, 48 photolyses). The set of ordinary differential equations is integrated with the KPP software package ([Sandu and Sander, 2006](#)), using the Rosenbrock method RODAS3. The release process of reactive halogens and the reactions with mercury and ozone both in the aerosol and the gas phase are shown in Fig. 1.

2.1 Gas phase oxidation reactions

Potential reactions of Hg in the atmosphere have recently been summarized by [Steffen et al. \(2008\)](#). The primary reactions include the oxidation by O₃ ([Pal and Ariya, 2004b](#); [Sumner, 2005](#)), the OH radical ([Sommar et al., 2001](#); [Pal and Ariya, 2004a](#)), H₂O₂ ([Tokos et al., 1998](#)) and reactive halogen species ([Ariya et al., 2002](#); [Calvert and Lindberg, 2003, 2004a](#); [Raofie and Ariya, 2003](#); [Donohoue et al., 2005, 2006](#); [Sumner, 2005](#)). Table 2 shows the reactions and their rate constants. There is a wide range of rate constants for GEM oxidation by O₃ and OH. Here, the temperature-dependent kinetic data reported by [Pal and Ariya \(2004a\)](#) and [Pal and Ariya \(2004b\)](#) are used.

Simulation of atmospheric mercury depletion events

Z.-Q. Xie et al.

Title Page

Abstract

Introduction

Conclusions

References

Tables

Figures

◀

▶

◀

▶

Back

Close

Full Screen / Esc

Printer-friendly Version

Interactive Discussion



**Simulation of
atmospheric mercury
depletion events**

Z.-Q. Xie et al.

Title Page

Abstract

Introduction

Conclusions

References

Tables

Figures

◀

▶

◀

▶

Back

Close

Full Screen / Esc

Printer-friendly Version

Interactive Discussion



The reactions of Hg with O₃ and OH are potentially important pathways for the loss of Hg in the continental troposphere, while in the marine boundary layer and the upper troposphere halogens are presumed to be dominant oxidants (Lin et al., 2006). The rate coefficients for the reactions of molecular halogens (Br₂ and Cl₂) and Br and Cl atoms and BrO with gas phase Hg atoms have been investigated (e.g., Ariya et al., 2002; Raofie and Ariya, 2003). Although the role of halogens in GEM destruction in the atmosphere is still uncertain and argued, it is known that reactions of Hg with Br₂, Cl₂, Br, Cl, and BrO are involved. There are only a few reports on the association reactions of HgBr with Br, Cl, BrO, and HgCl with Br and BrO radicals. The rate coefficients have not yet been determined experimentally. A value consistent with those measured for similar association reactions is assumed.

2.2 Aqueous phase redox chemistry

In contrast to the gas phase, aqueous-phase reactions of mercury include both oxidation and reduction (Table 3). Potential aqueous oxidants are O₃ (Munthe, 1992), the OH radical (Lin and Pehkonen, 1997), HOCl/ClO⁻ (Lin and Pehkonen, 1998), and Br₂/HOBr/BrO⁻ (Wang and Pehkonen, 2004). Compared to the gas phase, oxidation of Hg by O₃ and OH is very fast. Until the discovery of AMDEs in polar regions, it has thus commonly been thought that the main pathway for the conversion of Hg⁰ to Hg²⁺ is through aqueous-phase reactions. For the reduction of aqueous Hg²⁺, dissolved S(IV) (e.g., van Loon et al., 2000), HO₂ (Pehkonen and Lin, 1998) and the photolysis of Hg(OH)₂ are responsible. As the photolysis of Hg(OH)₂ is slow, its contribution should be small (Xiao et al., 1994). The reduction of aqueous Hg²⁺ by S(IV) was also reported to have a small rate constant (Munthe et al., 1991; van Loon et al., 2000). After depletion of aqueous S(IV), the reaction of HO₂ with Hg may be the only significant aqueous reduction balancing Hg⁰ oxidation (Lin and Pehkonen, 1998; Lin et al., 2006). However, there is no literature reporting a direct kinetic study of the Hg²⁺ + HO₂ reaction. Pehkonen and Lin (1998) proposed a two-step reduction of Hg²⁺ by HO₂ as

an important reducing pathway. For the second step, we assume the same value as for $\text{Hg}^+ + \text{OH}$.

2.3 Aqueous phase equilibria

Aqueous Hg^{2+} can form a wide variety of complexes with softer ligands such as Cl^- , Br^- , and SO_3^{2-} which have a significant impact on the reaction kinetics. Compared to these inorganic ligands, the concentrations of organic ligands are low and thus not considered here. Formation of Hg^{2+} complexes are treated as chemical equilibria since Hg^{2+} has a very rapid water exchange rate in aqueous solutions (Brezonik, 1994) (Table 4).

As suggested by Lin and Pehkonen (1997) and Lin and Pehkonen (1998), the total concentration of ligands and the pH of atmospheric droplets are important factors affecting Hg^{2+} speciation. At low S(IV) concentrations, the dominant complex is HgCl_2 (Lin et al., 2006), while at high S(IV) concentrations, the dominant complex is $\text{Hg}(\text{SO}_3)_2^{2-}$ (Lin and Pehkonen, 1998; Lin et al., 2006). Below pH 5.5, OH^- concentrations are low and can not form hydroxide complexes with Hg^{2+} . In the marine boundary layer or polar regions, the contribution of bromide (Br^-) complexes can be significant. Since the lifetime of aqueous S(IV) is only a few h, chloride and bromide may be the most important ligands resulting in the production of HgBr_2 and/or HgCl_2 (Lin et al., 2006).

2.4 Gas-aqueous phase exchange

Equilibration towards Henry's law is calculated using the mass-transfer coefficients (k_{mt}) according to Schwartz (1986). The accommodation coefficient was assumed to be $\alpha=0.1$ for all mercury species, and the Henry's law coefficients are listed in Table 5. Mercury compounds have vapor pressures orders of magnitude lower than that of elemental mercury and belong to the group of semivolatiles.

Simulation of atmospheric mercury depletion events

Z.-Q. Xie et al.

Title Page

Abstract

Introduction

Conclusions

References

Tables

Figures

◀

▶

◀

▶

Back

Close

Full Screen / Esc

Printer-friendly Version

Interactive Discussion



3 Results and discussion

The conditions of our model runs are similar to those in [Sander et al. \(2006\)](#). The model starts on 31 March with initial gas-phase mixing ratios as shown in Table 6. The temperature is set to $T=240$ K. Photolysis rate coefficients are calculated for a latitude of 82° N. Sea salt particles (2μ m radius) are injected into the air on 4 April (i.e. after a spin up of 4 days). They are composed of well-mixed, liquid, concentrated sea water ($c=5$ mol/L), assuming that 30% of the carbonate has precipitated before particle formation. The initial liquid water content (LWC) of the model aerosol is 5×10^{-10} m^3/m^3 , and it decays exponentially with a lifetime of 3 days. The main features of this BASE run, and also of several sensitivity studies (as described in the sections below) are summarized in Table 7.

After injection into the air, the aerosol pH drops abruptly to about 3. The so-called “bromine explosion” starts and the levels of BrO and Br increase quickly. Sea salt aerosol is depleted in Br^- during this period. After 2 days both Hg and O_3 are thoroughly depleted.

3.1 Model-calculated speciation of mercury compounds

Potential oxidation products of gaseous Hg include HgO, HgCl, HgCl₂, HgBr, HgBr₂, ClHgBr, BrHgOBr and ClHgOBr. Their modeled levels during the AMDE are shown in Fig. 2. HgCl and HgBr are intermediates and only found during the first two days. HgO also disappears after two days. The major Hg-containing product is BrHgOBr. Our modeled speciation is in agreement with results by [Calvert and Lindberg \(2003\)](#). After two days the total of oxidized gaseous mercury peaks around 0.1 pmol/mol. The maxima of HgCl₂ and HgBr₂ at the end of the AMDE only reach 0.0075 and 0.015 pmol/mol, respectively. [Lindberg et al. \(2002\)](#) reported that more than 0.9 ng/m³ (1 ng/m³ equals 0.11 pmol/mol) of oxidized gaseous mercury quickly deposited during AMDEs at Barrow. Therefore, the model predictions are generally consistent with ambient observations. However, it should be noted that dry deposition of gas-phase species was

Simulation of atmospheric mercury depletion events

Z.-Q. Xie et al.

Title Page

Abstract

Introduction

Conclusions

References

Tables

Figures

◀

▶

◀

▶

Back

Close

Full Screen / Esc

Printer-friendly Version

Interactive Discussion



switched off in the model, and thus the loss of RGM is entirely due to uptake into the aerosol and subsequent aerosol loss.

The main mercury species in the aqueous phase are BrHgOBr , HgBr_2 , and HgCl_2 . At the beginning of the AMDE, the levels of halogen complexes increase quickly and peak when GEM reaches zero (except for the intermediates HgCl^+ and HgBr^+). After that, their amount in the atmosphere decreases (Fig. 3, in mol/mol) due to the loss of sea salt aerosols, while their aqueous-phase concentrations reach equilibria and remain constant (Fig. 4, in mol/L).

The main sulfur complexes are HgSO_3 and $\text{Hg}(\text{SO}_3)_2^{2-}$. Their concentrations are very low and their diurnal cycles after AMDEs are controlled by the variation of SO_3^{2-} concentrations. In contrast to the study by Pan and Carmichael (2005), the sum of all divalent mercury complexes ($\text{Hg}_{\text{tot}}^{2+}$) does not display a diurnal cycle. We have performed further sensitivity tests to find the reason for this difference. As shown in Fig. 5 (top row), when bromine chemistry was switched off, neither $\text{Hg}_{\text{tot}}^{2+}$ nor HgCl_2 show a diurnal cycle. This is due to the high levels of Cl^- in the sea-salt aerosol of our model. When both chlorine and bromine chemistry were switched off, $\text{Hg}_{\text{tot}}^{2+}$ concentrations display the same cycle as calculated by Pan and Carmichael (2005), which is controlled by the oxygen-hydrogen photochemical reactions that produce HO_2 radicals in the liquid phase (Fig. 5, bottom row).

To the best of our knowledge, this is the first model study of atmospheric mercury speciation in both the gas and the aqueous phase including bromine chemistry. However, our results can only be considered preliminary because we had to use estimates for several Henry's law coefficients. Still, we hope that our simulations can provide first clues about the mercury compounds deposited to the snowpack in polar regions.

3.2 The reactions of Hg with Br and BrO

Both Br and BrO are considered potentially important reactants responsible for the observed loss of GEM in polar regions during bromine explosions. However, the

Simulation of atmospheric mercury depletion events

Z.-Q. Xie et al.

Title Page

Abstract

Introduction

Conclusions

References

Tables

Figures

◀

▶

◀

▶

Back

Close

Full Screen / Esc

Printer-friendly Version

Interactive Discussion



**Simulation of
atmospheric mercury
depletion events**

Z.-Q. Xie et al.

Title Page

Abstract

Introduction

Conclusions

References

Tables

Figures

◀

▶

◀

▶

Back

Close

Full Screen / Esc

Printer-friendly Version

Interactive Discussion

kinetics are not well-known, and a wide range of rate coefficients has been published for their reactions. Holmes et al. (2006) compiled literature values of the rate coefficient $k_{\text{Hg}+\text{Br}}$. At 1 atm and 298 K, it is between $3.0\text{--}9.7\times 10^{-13}$ (Donohoue et al., 2006) and $3.2\times 10^{-12}\text{ cm}^3\text{ mol}^{-1}\text{ s}^{-1}$ (Ariya et al., 2002). There is limited information about its temperature- and pressure-dependence. Khalizov et al. (2003) and Goodsite et al. (2004) reported values of $1.0\times 10^{-12}\text{ exp}(209\text{ K}/T)$ and $1.1\times 10^{-12}(T/298\text{ K})^{-2.37}\text{ cm}^3\text{ mol}^{-1}\text{ s}^{-1}$, respectively, at 1 atm. Regarding the reaction $\text{Hg}+\text{BrO}$, Holmes et al. (2006) and Shepler et al. (2007) argued, based upon theoretical calculations, that it is unlikely to occur in the atmosphere as it is endothermic and has a large energy barrier. However, laboratory measurements by Raofie and Ariya (2003) showed that $k_{\text{Hg}+\text{BrO}}$ is between 10^{-15} and $10^{-13}\text{ cm}^3\text{ mol}^{-1}\text{ s}^{-1}$. Further experiments identified HgBr, HgBrO/HgOBr, and HgO as reaction products (Raofie and Ariya, 2004). To test the possible importance of $\text{Hg}+\text{Br}$ and $\text{Hg}+\text{BrO}$ in our model, we have performed several sensitivity runs, varying their rate coefficients.

In a first series of simulations, the reaction $\text{Hg}+\text{BrO}$ is switched off, and $k_{\text{Hg}+\text{Br}}$ is varied (top graph in Fig. 6). With $k_{\text{Hg}+\text{Br}}=1.0\times 10^{-14}$, 1.0×10^{-13} , 3.0×10^{-13} , 1.0×10^{-13} , $3.2\times 10^{-12}\text{ cm}^3\text{ mol}^{-1}\text{ s}^{-1}$, a fraction of 5.0%, 30%, 65%, 97% and 100% mercury, respectively, has been depleted after one day. In a second series, the reaction $\text{Hg}+\text{Br}$ is switched off, and $k_{\text{Hg}+\text{BrO}}$ is varied (bottom graph in Fig. 6). With $k_{\text{Hg}+\text{BrO}}=1.0\times 10^{-15}$, 5.0×10^{-15} , 1.0×10^{-14} , 5.0×10^{-14} , $1.0\times 10^{-13}\text{ cm}^3\text{ mol}^{-1}\text{ s}^{-1}$, a fraction of 7.0%, 29%, 52%, 97% and 100% mercury, respectively, has been depleted after one day.

Calvert and Lindberg (2003) suggested that if the rate coefficient $k_{\text{Hg}+\text{BrO}}$ is at least 1/30th to 1/450th of $k_{\text{Hg}+\text{Br}}$, then reaction of Hg with BrO can be as important as that with Br atoms. We performed further sensitivity runs to study the relative importance of these reactions. The results are shown in Fig. 7. In agreement with Calvert and Lindberg (2003), changing the mercury-related rate coefficients does not affect ozone or bromine species significantly. When both $k_{\text{Hg}+\text{Br}}$ and $k_{\text{Hg}+\text{BrO}}$ are zero (solid black line in Fig. 7), only 1.3% of the initial Hg is depleted during the first day, showing that

in polar regions the reactions with O_3 , OH, H_2O_2 , Br_2 , Cl_2 , or Cl are not sufficient to deplete GEM. Also shown in the figure are the temporal evolution of Br and BrO during the ODE. Due to the ozone depletion, there is a steady increase in the ratio Br/BrO. Thus the relative importance of $Hg+BrO$ and $Hg+Br$ will shift towards the latter during the AMDE. In the beginning, when O_3 decreases, the ratio is small with high levels of BrO, while when O_3 is low, less BrO is produced and subsequently the ratio increases.

This can be seen clearly in Fig. 8, which shows a model simulation of an ODE that lasts several days. The reaction $Hg+Br$ is important throughout the ODE, whereas the reaction $Hg+BrO$ slows down towards the end of the ODE, and never exceeds 10% of the total Hg loss rate. Both reactions show diurnal cycles with faster rates during the day. The diurnal cycle of $Hg+Br$ is more pronounced than that of $Hg+BrO$.

It is interesting to compare the loss rates of Hg and O_3 . Ebinghaus et al. (2002) reported Antarctic measurements with 15-min resolution and found a highly significant correlation between TGM and O_3 at a lag-time of zero. In our model calculations, such a synchronous loss of GEM and ozone can best be reproduced when using $k_{Hg+Br}=3.0\times 10^{-13}$ and $k_{Hg+BrO}\leq 1.0\times 10^{-15} \text{ cm}^3 \text{ mol}^{-1} \text{ s}^{-1}$. Using these rate coefficients for different mercury depletion scenarios, our model results show a significant correlation between mercury and ozone ($R^2=0.97$, see Fig. 9)

With other values of k_{Hg+Br} , the rate of GEM destruction will either be faster or slower than that of O_3 (Figs. 6 and 7).

In the model runs where the reaction $Hg+Br$ is switched off and the loss of GEM is due to reaction with BrO, a synchronized loss of Hg and O_3 cannot be reproduced. When $k_{Hg+BrO} > 1.0\times 10^{-14} \text{ cm}^3 \text{ s}^{-1}$, Hg loss is faster than that of ozone. With smaller values of k_{Hg+BrO} , the reaction becomes too slow towards the end of the ODE, when the concentration of Hg is small and the Br/BrO ratio is high (Figs. 6 and 7). This implies that the contribution of $Hg+BrO$ to AMDEs is small.

Simulation of atmospheric mercury depletion events

Z.-Q. Xie et al.

Title Page

Abstract

Introduction

Conclusions

References

Tables

Figures

◀

▶

◀

▶

Back

Close

Full Screen / Esc

Printer-friendly Version

Interactive Discussion



3.3 Effects of temperature

Variations in temperature have a strong effect on reaction kinetics. For most reactions of mercury species, the temperature-dependence of the rate coefficients is not known. Still, models can be used to study indirect effects resulting from temperature effects on sulfur and halogen species.

Pan and Carmichael (2005) simulated the effect of temperature in the aqueous phase at night without halogens. In their model, low temperatures slow the oxidation of mercury in the aqueous phase and increase the time for the system to reach equilibrium. High temperatures favor the partitioning of H_2SO_3 into SO_3^{2-} , and increase the oxidation rate of SO_3^{2-} . The net result is that the SO_3^{2-} elimination speed is greater than its production speed. Therefore, they concluded that higher temperatures result in lower concentrations of SO_3^{2-} , and favor the liquid-phase mercury oxidation reactions.

However, another effect that has to be considered is the temperature-dependence of the bromine explosion. Sander et al. (2006) simulated the role of temperature in the activation of bromine. They found that low temperatures favor the activation of reactive bromine due to a shift of the equilibrium between BrCl and Br_2Cl^- . An increase in bromine enhances the oxidation of Hg.

To study these counteracting effects, we performed model runs at $T=298\text{ K}$ and 240 K , as shown in Fig. 10. Consistent with the results from Pan and Carmichael (2005), the initial loss of Hg (before the bromine explosion) is faster at 298 K . However, once the ODE starts, the loss of Hg is more pronounced at 240 K because of the higher concentrations of bromine species.

4 Conclusions

Investigating the chemistry of AMDEs with MECCA, we found that:

1. The reaction of Hg with Br dominates the loss of GEM throughout the depletion event. To explain the experimentally observed synchronous destruction

Simulation of atmospheric mercury depletion events

Z.-Q. Xie et al.

Title Page

Abstract

Introduction

Conclusions

References

Tables

Figures

⏪

⏩

◀

▶

Back

Close

Full Screen / Esc

Printer-friendly Version

Interactive Discussion



**Simulation of
atmospheric mercury
depletion events**

Z.-Q. Xie et al.

Title Page

Abstract

Introduction

Conclusions

References

Tables

Figures

◀

▶

◀

▶

Back

Close

Full Screen / Esc

Printer-friendly Version

Interactive Discussion

of Hg and O₃, the reaction rate of Hg+BrO has to be much lower than that of Hg+Br. The synchronicity is best reproduced with rate coefficients at the lower limit of the literature values for both reactions, i.e. $k_{\text{Hg+Br}} \approx 3 \times 10^{-13}$ and $k_{\text{Hg+BrO}} \leq 1 \times 10^{-15} \text{ cm}^3 \text{ mol}^{-1} \text{ s}^{-1}$, respectively.

2. BrHgOBr is the most abundant reactive mercury species, both in the gas phase and in the aqueous phase. The aqueous phase concentrations of BrHgOBr, HgBr₂, and HgCl₂ are several orders of magnitude larger than that of Hg(SO₃)₂²⁻. Note, however, that these results depend on the assumed Henry's law coefficients, which need to be confirmed by measurements.
3. Considering chlorine chemistry outside depletion events (i.e. without bromine activation), the concentration of total divalent mercury in the sea-salt aerosol (concentrated solution droplets) is dominated by HgCl₂, does not exhibit a diurnal cycle, and is much higher than in dilute aqueous solution droplets, where it is dominated by Hg(SO₃)₂²⁻ and negatively correlated with the HO₂ radical concentration.

Acknowledgements. The Max-Planck Society and M. O. Andreae are gratefully acknowledged for support. Z.-Q. Xie acknowledges financial support from the Alexander von Humboldt Foundation and from the Chinese National Natural Science Foundation (grant no. 40776001) to visit Germany.

References

- Ariya, P. A., Khalizov, A., and Gidas, A.: Reactions of gaseous mercury with atomic and molecular halogens: Kinetics, product studies, and atmospheric implications, *J. Phys. Chem. A*, 106, 7310–7320, 2002. [13199](#), [13201](#), [13202](#), [13206](#), [13218](#)
- Ariya, P. A., Dastoor, A. P., Amyot, M., Schroeder, W. H., Barrie, L., Anlauf, K., Raofie, F., Ryzhkov, A., Davignon, D., Lalonde, J., and Steffen, A.: The Arctic: a sink for mercury, *Tellus*, 56B, 397–403, 2004. [13199](#)



**Simulation of
atmospheric mercury
depletion events**

Z.-Q. Xie et al.

Title Page

Abstract

Introduction

Conclusions

References

Tables

Figures

◀

▶

◀

▶

Back

Close

Full Screen / Esc

Printer-friendly Version

Interactive Discussion

- Barrie, L. A., Bottenheim, J. W., Schnell, R. C., Crutzen, P. J., and Rasmussen, R. A.: Ozone destruction and photochemical reactions at polar sunrise in the lower Arctic atmosphere, *Nature*, 334, 138–141, 1988. [13199](#)
- Berg, T., Sekkesæter, S., Steinnes, E., Valdal, A.-K., and Wibetoe, G.: Springtime depletion of mercury in the European Arctic as observed at Svalbard, *Sci. Total Environ.*, 304, 43–51, 2003. [13199](#)
- Bottenheim, J. W., Gallant, A. G., and Brice, K. A.: Measurements of NO_y species and O₃ at 82° N latitude, *Geophys. Res. Lett.*, 13, 113–116, 1986. [13199](#)
- Brezonik, P. L.: *Chemical Kinetics and Process Dynamics in Aquatic Systems*, CRC Press, Boca Raton, FL, 1994. [13203](#)
- Calvert, J. G. and Lindberg, S. E.: A modeling study of the mechanism of the halogen-ozone-mercury homogeneous reactions in the troposphere during the polar spring, *Atmos. Environ.*, 37, 4467–4481, 2003. [13200](#), [13201](#), [13204](#), [13206](#), [13217](#), [13218](#)
- Calvert, J. G. and Lindberg, S. E.: Potential influence of iodine-containing compounds on the chemistry of the troposphere in the polar spring. I. Ozone depletion, *Atmos. Environ.*, 38, 5087–5104, 2004a. [13199](#), [13201](#)
- Calvert, J. G. and Lindberg, S. E.: The potential influences of iodine containing compounds on the chemistry of the troposphere in the polar spring II, *Atmos. Environ.*, 38, 5105–5116, 2004b. [13199](#)
- Canosa-Mas, C. E., King, M. D., Lopez, R., Percival, C. J., Wayne, R. P., Shallcross, D. E., Pyle, J. A., and Daele, V.: Is the reaction between CH₃(O)O₂ and NO₃ important in the night-time troposphere?, *J. Chem. Soc. Faraday Trans.*, 92, 2211–2222, 1996. [13200](#)
- Christensen, J. H., Brandt, J., Frohn, L. M., and Skov, H.: Modelling of mercury in the Arctic with the Danish Eulerian Hemispheric Model, *Atmos. Chem. Phys.*, 4, 2251–2257, 2004, <http://www.atmos-chem-phys.net/4/2251/2004/>. [13200](#), [13217](#)
- Clever, H. L., Johnson, S. A., and Derrick, M. E.: The solubility of mercury and some sparingly soluble mercury salts in water and aqueous-electrolyte solutions, *J. Phys. Chem. Ref. Data*, 14, 631–681, 1985. [13220](#)
- Dastoor, A. P. and Larocque, Y.: Global circulation of atmospheric mercury: a modeling study, *Atmos. Environ.*, 38, 147–161, 2004. [13200](#), [13217](#)
- Donohoue, D. L., Bauer, D., and Hynes, A. J.: Temperature and pressure dependent rate coefficients for the reaction of Hg with Cl and the reaction of Cl with Cl: a pulsed laser photolysis-pulsed laser induced fluorescence study, *J. Phys. Chem. A.*, 109, 7732–7741, 2005. [13201](#)



**Simulation of
atmospheric mercury
depletion events**

Z.-Q. Xie et al.

Title Page

Abstract

Introduction

Conclusions

References

Tables

Figures

◀

▶

◀

▶

Back

Close

Full Screen / Esc

Printer-friendly Version

Interactive Discussion



Donohoue, D. L., Bauer, D., Cossairt, B., and Hynes, A. J.: Temperature and pressure dependent rate coefficients for the reaction of Hg with Br and the reaction of Br with Br: a pulsed laser photolysis-pulsed laser induced fluorescence study, *J. Phys. Chem. A.*, 110, 6623–6632, 2006. [13201](#), [13206](#), [13218](#)

5 Ebinghaus, R., Kock, H. H., Temme, C., Einax, J. W., Löwe, A. G., Richter, A., Burrows, J. P., and Schroeder, W. H.: Antarctic springtime depletion of atmospheric mercury, *Environ. Sci. Technol.*, 36, 1238–1244, 2002. [13199](#), [13207](#)

Goodsite, M., Plane, J. M. C., and Skov, H.: A theoretical study of the oxidation of Hg⁰ to HgBr₂ in the troposphere, *Environ. Sci. Technol.*, 38, 1772–1776, 2004. [13199](#), [13206](#)

10 Hedgecock, I. M., Trunfio, G. A., Pirrone, N., and Sprovieri, F.: Mercury chemistry in the MBL: Mediterranean case and sensitivity studies using the AMCOTS (Atmospheric Mercury Chemistry over the Sea) model, *Atmos. Environ.*, 39, 7217–7230, 2005. [13200](#), [13217](#)

Holmes, C. D., Jacob, D. J., and Yang, X.: Global lifetime of elemental mercury against oxidation by atomic bromine in the free troposphere, *Geophys. Res. Lett.*, 33, L20808, doi:10.1029/2006GL027176, 2006. [13206](#)

15 Khalizov, A. F., Viswanathan, B., Larregaray, P., and Ariya, P. A.: A theoretical study on the reactions of Hg with halogens: Atmospheric implications, *J. Phys. Chem. A*, 107, 6360–6365, 2003. [13206](#)

Lin, C.-J. and Pehkonen, S. O.: Aqueous free radical chemistry of mercury in the presence of iron oxides and ambient aerosol, *Atmos. Environ.*, 31, 4125–4137, 1997. [13202](#), [13203](#), [13219](#)

Lin, C.-J. and Pehkonen, S. O.: Oxidation of elemental mercury by aqueous chlorine (HOCl/OCl⁻): Implications for tropospheric mercury chemistry, *J. Geophys. Res.*, 103D, 28 093–28 102, 1998. [13202](#), [13203](#), [13219](#)

25 Lin, C.-J., Pongprueksa, P., Lindberg, S. E., Pehkonen, S. O., Byune, D., and Jang, C.: Scientific uncertainties in atmospheric mercury models I: Model science evaluation, *Atmos. Environ.*, 40, 2911–2928, 2006. [13202](#), [13203](#)

Lindberg, S. E., Brooks, S., Lin, C.-J., Scott, K., Meyers, T., Chambers, L., Landis, M., and Stevens, R.: Formation of reactive gaseous mercury in the Arctic: Evidence of oxidation of Hg⁰ to gas-phase Hg–II compounds after Arctic sunrise, *Water Air Soil Pollut. Focus*, 1, 295–302, 2001. [13199](#)

30 Lindberg, S. E., Brooks, S., Lin, C.-J., Scott, K. J., Landis, M. S., Stevens, R. K., Goodsite, M., and Richter, A.: Dynamic oxidation of gaseous mercury in the Arctic troposphere at polar

- sunrise, *Environ. Sci. Technol.*, 36, 1245–1256, 2002. [13199](#), [13204](#)
- Lu, J. Y. and Schroeder, W. H.: Annual time-series of total filterable atmospheric mercury concentrations in the Arctic, *Tellus*, 56B, 213–222, 2004. [13199](#)
- Lu, J. Y., Schroeder, W. H., Barrie, L. A., Steffen, A., Welch, H. E., Martin, K., Lockhart, L.,
5 Hunt, R. V., Boila, G., and Richter, A.: Magnification of atmospheric mercury deposition to polar regions in springtime: the link to tropospheric ozone depletion chemistry, *Geophys. Res. Lett.*, 28, 3219–3222, 2001. [13199](#)
- Munthe, J.: The aqueous oxidation of elemental mercury by ozone, *Atmos. Environ.*, 26A, 1461–1468, 1992. [13202](#), [13219](#)
- 10 Munthe, J., Xiao, Z. F., and Lindqvist, O.: The aqueous reduction of divalent mercury by sulfite, *Water Air Soil Pollut.*, 56, 621–630, 1991. [13202](#)
- Pal, B. and Ariya, P. A.: Gas-phase HO-initiated reactions of elemental mercury: Kinetics, product studies, and atmospheric implications, *Environ. Sci. Technol.*, 38, 5555–5566, 2004a. [13201](#), [13218](#)
- 15 Pal, B. and Ariya, P. A.: Studies of ozone initiated reactions of gaseous mercury: Kinetics, product studies, and atmospheric implications, *Phys. Chem. Chem. Phys.*, 6, 572–579, 2004b. [13201](#), [13218](#)
- Pan, L. and Carmichael, G. R.: A two-phase box model to study mercury atmospheric mechanisms, *Environ. Chem.*, 2, 205–214, 2005. [13200](#), [13205](#), [13208](#), [13217](#), [13220](#)
- 20 Pehkonen, S. O. and Lin, C. J.: Aqueous photochemistry of divalent mercury with organic acids, *J. Air Waste Manage. Assoc.*, 48, 144–150, 1998. [13202](#), [13219](#)
- Perovich, D. K. and Richter-Menge, J. A.: Surface characteristics of lead ice, *J. Geophys. Res.*, 99C, 16 341–16 350, 1994. [13200](#)
- Petersen, G., Munthe, J., Pleijel, K., Bloxam, R., and Kumar, A. V.: A comprehensive Eulerian modeling framework for airborne mercury species: Development and testing of the tropospheric chemistry module (TCM), *Atmos. Environ.*, 32, 829–843, 1998. [13200](#)
- 25 Pleijel, K. and Munthe, J.: Modelling the atmospheric mercury cycle — Chemistry in fog droplets, *Atmos. Environ.*, 29, 1441–1457, 1995. [13219](#)
- Poissant, L. and Pilote, M.: Time series analysis of atmospheric mercury in Kuujuaupik/Whapmagoostui (Québec), *J. Phys. IV France*, 107, 1079–1082, 2003. [13199](#)
- 30 Rankin, A. M., Wolff, E. W., and Martin, S.: Frost flowers: Implications for tropospheric chemistry and ice core interpretation, *J. Geophys. Res.*, 107, 4683, doi:10.1029/2002JD002492, 2002. [13200](#)

**Simulation of
atmospheric mercury
depletion events**Z.-Q. Xie et al.

Title Page

Abstract

Introduction

Conclusions

References

Tables

Figures

◀

▶

◀

▶

Back

Close

Full Screen / Esc

Printer-friendly Version

Interactive Discussion



**Simulation of
atmospheric mercury
depletion events**

Z.-Q. Xie et al.

Title Page

Abstract

Introduction

Conclusions

References

Tables

Figures

◀

▶

◀

▶

Back

Close

Full Screen / Esc

Printer-friendly Version

Interactive Discussion



- Raofie, F. and Ariya, P. A.: Kinetics and products study of the reaction of BrO radicals with gaseous mercury, *J. Phys. IV France*, 107, 1119–1121, 2003. [13201](#), [13202](#), [13206](#), [13218](#)
- Raofie, F. and Ariya, P. A.: Product study of the gas-phase BrO-initiated oxidation of Hg⁰: Evidence for stable Hg¹⁺ compounds, *Environ. Sci. Technol.*, 38, 4319–4326, 2004. [13206](#)
- 5 Ryaboshapko, A., Bullock, R., Ebinghaus, R., Ilyin, I., Lohman, K., Munthe, J., Petersen, G., Seigneur, C., and Wängberg, I.: Comparison of mercury chemistry models, *Atmos. Environ.*, 36, 3881–3898, 2002. [13200](#)
- Sander, R., Kerkweg, A., Jöckel, P., and Lelieveld, J.: Technical Note: The new comprehensive atmospheric chemistry module MECCA, *Atmos. Chem. Phys.*, 5, 445–450, 2005, <http://www.atmos-chem-phys.net/5/445/2005/>. [13201](#)
- 10 Sander, R., Burrows, J., and Kaleschke, L.: Carbonate precipitation in brine – a potential trigger for tropospheric ozone depletion events, *Atmos. Chem. Phys.*, 6, 4653–4658, 2006, <http://www.atmos-chem-phys.net/6/4653/2006/>. [13200](#), [13201](#), [13204](#), [13208](#)
- Sandu, A. and Sander, R.: Technical Note: Simulating chemical systems in Fortran90 and Matlab with the kinetic preprocessor KPP-2.1, *Atmos. Chem. Phys.*, 6, 187–195, 2006, <http://www.atmos-chem-phys.net/6/187/2006/>. [13201](#)
- 15 Schroeder, W. H. and Munthe, J.: Atmospheric mercury – An overview, *Atmos. Environ.*, 32, 809–822, 1998. [13221](#)
- Schroeder, W. H., Anlauf, K. G., Barrie, L. A., Lu, J. Y., Steffen, A., Schneeberger, D. R., and Berg, T.: Arctic springtime depletion of mercury, *Nature*, 394, 331–332, 1998. [13199](#)
- 20 Schwartz, S. E.: Mass-transport considerations pertinent to aqueous phase reactions of gases in liquid-water clouds, in: *Chemistry of Multiphase Atmospheric Systems*, NATO ASI Series, Vol. G6, edited by Jaeschke, W., 415–471, Springer Verlag, Berlin, 1986. [13203](#)
- Shepler, B. C., Balabanov, N. B., and Peterson, K. A.: Hg+Br–HgBr recombination and collision-induced dissociation dynamics, *J. Phys. Chem.*, 127, 164–304, 2007. [13206](#)
- 25 Shon, Z.-H., Kim, K.-H., Kim, M.-Y., and Lee, M.: Modeling study of reactive gaseous mercury in the urban air, *Atmos. Environ.*, 39, 749–761, 2005. [13200](#), [13217](#), [13221](#)
- Simpson, W. R., von Glasow, R., Riedel, K., Anderson, P., Ariya, P., Bottenheim, J., Burrows, J., Carpenter, L. J., Frieß, U., Goodsite, M. E., Heard, D., Hutterli, M., Jacobi, H.-W., Kaleschke, L., Neff, B., Plane, J., Platt, U., Richter, A., Roscoe, H., Sander, R., Shepson, P., Sodeau, J., Steffen, A., Wagner, T., and Wolff, E.: Halogens and their role in polar boundary-layer ozone depletion, *Atmos. Chem. Phys.*, 7, 4375–4418, 2007, <http://www.atmos-chem-phys.net/7/4375/2007/>. [13199](#), [13200](#)

**Simulation of
atmospheric mercury
depletion events**Z.-Q. Xie et al.

Title Page

Abstract

Introduction

Conclusions

References

Tables

Figures

◀

▶

◀

▶

Back

Close

Full Screen / Esc

Printer-friendly Version

Interactive Discussion



- Skov, H., Christensen, J. H., Goodsite, M. E., Heidam, N. Z., Jensen, B., Wåhlin, P., and Geernaert, G.: Fate of elemental mercury in the Arctic during atmospheric mercury depletion episodes and the load of atmospheric mercury to the Arctic, *Environ. Sci. Technol.*, 38, 2373–2382, 2004. [13199](#), [13200](#), [13217](#)
- 5 Slemr, F., Brunke, E., Ebinghaus, R., Temme, C., Munthe, J., Wangberg, I., Schroeder, W. H., Steffen, A., and Berg, T.: Worldwide trend of atmospheric mercury since 1977, *Geophys. Res. Lett.*, 30, doi:10.1029/2003GL016954, 2003. [13199](#)
- Sommar, J., Gardfeldt, K., Stromberg, D., and Feng, X.: A kinetic study of the gas-phase reaction between the hydroxyl radical and atomic mercury, *Atmos. Environ.*, 35, 3049–3054, 2001. [13201](#)
- 10 Sprovieri, F., Pirrone, N., Hedgecock, I. M., Landis, M. S., and Stevens, R. K.: Intensive atmospheric mercury measurements at Terra Nova Bay in Antarctica during November and December 2000, *J. Geophys. Res.*, 107D, 4722, doi:10.1029/2002JD002057, 2002. [13199](#)
- Steffen, A., Douglas, T., Amyot, M., Ariya, P., Aspmo, K., Berg, T., Bottenheim, J., Brooks, S., Cobbett, F., Dastoor, A., Dommergue, A., Ebinghaus, R., Ferrari, C., Gardfeldt, K., Goodsite, M. E., Lean, D., Poulain, A. J., Scherz, C., Skov, H., Sommar, J., and Temme, C.: A synthesis of atmospheric mercury depletion event chemistry in the atmosphere and snow, *Atmos. Chem. Phys.*, 8, 1445–1482, 2008, <http://www.atmos-chem-phys.net/8/1445/2008/>. [13199](#), [13201](#)
- 15 Sumner, A. L.: *Where We Stand on Mercury Pollution and its Health Effects on Regional and Global Scales*, Springer US, 2005. [13201](#)
- Temme, C., Einax, J. W., Ebinghaus, R., and Schroeder, W. H.: Measurements of atmospheric mercury species at a coastal site in the Antarctic and over the South Atlantic Ocean during polar summer, *Environ. Sci. Technol.*, 37, 22–31, 2003. [13199](#)
- 20 Tokos, J. J. S., Hall, B., Calhoun, J. A., and Prestbo, E. M.: Homogeneous gas-phase reaction of Hg^0 with H_2O_2 , O_3 , CH_3I , and $(\text{CH}_3)_2\text{S}$: Implications for atmospheric Hg cycling, *Atmos. Environ.*, 32, 823–827, 1998. [13201](#), [13218](#)
- Travnikov, O.: Contribution of the intercontinental atmospheric transport to mercury pollution in the Northern Hemisphere, *Atmos. Environ.*, 39, 7541–7548, 2005. [13200](#), [13217](#)
- 25 van Loon, L., Mader, E., and Scott, S. L.: Reduction of the aqueous mercuric ion by sulfite: UV spectrum of HgSO_3 and its intramolecular redox reaction, *J. Phys. Chem. A*, 104, 1621–1626, 2000. [13202](#), [13219](#)
- van Loon, L. L., Mader, E. A., and Scott, S. L.: Sulfite stabilization and reduction of the aqueous

mercuric ion: Kinetic determination of sequential formation constants, *J. Phys. Chem. A*, 105, 3190–3195, 2001. [13220](#)

Wang, Z. and Pehkonen, S. O.: Oxidation of elemental mercury by aqueous bromine: atmospheric implications, *Atmos. Environ.*, 38, 3675–3688, 2004. [13202](#), [13219](#)

Xiao, Z. F., Munthe, J., Stromberg, D., and Lindqvist, O.: Photochemical behavior of inorganic mercury compounds in aqueous solution, in: *Mercury as a Global Pollutant – Integration and Synthesis*, edited by: Watras, C. J. and Huckabee, J. W., 581–592, Lewis Publishers, 1994. [13202](#), [13219](#)

ACPD

8, 13197–13233, 2008

Simulation of atmospheric mercury depletion events

Z.-Q. Xie et al.

Title Page

Abstract

Introduction

Conclusions

References

Tables

Figures

◀

▶

◀

▶

Back

Close

Full Screen / Esc

Printer-friendly Version

Interactive Discussion



Simulation of atmospheric mercury depletion events

Z.-Q. Xie et al.

Table 1. Comparison of mercury models with halogen chemistry.

Br	Cl	aqueous phase	mass transfer	region	reference
–	+	+	dynamic (k_{mt})	Northern Hemisphere	Christensen et al. (2004)
–	+	+	equilibrium	Northern Hemisphere	Travnikov (2005)
–	+	+	dynamic (k_{mt})	global	Dastoor and Larocque (2004)
+	+	–	–	polar	Calvert and Lindberg (2003)
+	+	–	–	Northern Hemisphere	Skov et al. (2004)
–	+	dilute droplets	equilibrium	unspecified	Pan and Carmichael (2005)
+	+	aerosol	dynamic (k_{mt})	Mediterranean	Hedgecock et al. (2005)
+	+	aerosol	dynamic (k_{mt})	urban	Shon et al. (2005)
+	+	aerosol	dynamic (k_{mt})	polar	this work

Title Page

Abstract

Introduction

Conclusions

References

Tables

Figures

◀

▶

◀

▶

Back

Close

Full Screen / Esc

Printer-friendly Version

Interactive Discussion



Simulation of atmospheric mercury depletion events

Z.-Q. Xie et al.

Table 2. Gas-phase reactions.

	k [cm ³ mol ⁻¹ s ⁻¹]	reference
Hg+O ₃ →HgO+O ₂	8.43E-17×exp(-1407K/T)	Pal and Ariya (2004b)
Hg+OH→HgO+H	3.55E-14×exp(294K/T)	Pal and Ariya (2004a)
Hg+H ₂ O ₂ →HgO+H ₂ O	8.5E-19	Tokos et al. (1998)
Hg+Cl→HgCl	1.0E-11	Ariya et al. (2002)
Hg+Cl ₂ →HgCl ₂	2.6E-18	Ariya et al. (2002)
Hg+Br→HgBr	3.0E-13	Donohoue et al. (2006)
HgBr+Br→HgBr ₂	3.0E-12	Calvert and Lindberg (2003)
Hg+Br ₂ →HgBr ₂	9.0E-17	Ariya et al. (2002)
Hg+BrO→HgO+Br	1.0E-15	Raofie and Ariya (2003)
HgBr+BrO→BrHgOBr	3.0E-12	see note*
HgCl+BrO→ClHgOBr	3.0E-12	see note*
HgBr+Cl→ClHgBr	3.0E-12	see note*
HgCl+Br→ClHgBr	3.0E-12	see note*

* We have used the value k (HgBr+Br) here, as assumed by Calvert and Lindberg (2003).

Title Page

Abstract

Introduction

Conclusions

References

Tables

Figures

◀

▶

◀

▶

Back

Close

Full Screen / Esc

Printer-friendly Version

Interactive Discussion



Simulation of atmospheric mercury depletion events

Z.-Q. Xie et al.

Title Page

Abstract

Introduction

Conclusions

References

Tables

Figures

◀

▶

◀

▶

Back

Close

Full Screen / Esc

Printer-friendly Version

Interactive Discussion

Table 3. Aqueous-phase reactions.

	k		reference
$\text{Hg} + \text{O}_3 \rightarrow \text{HgO} + \text{O}_2$	4.7E7	$\text{M}^{-1}\text{s}^{-1}$	Munthe (1992)
$\text{HgO} + \text{H}^+ \rightarrow \text{Hg}^{2+} + \text{OH}^-$	1.0E10	$\text{M}^{-1}\text{s}^{-1}$	Pleijel and Munthe (1995)
$\text{Hg} + \text{OH} \rightarrow \text{Hg}^+ + \text{OH}^-$	2.0E9	$\text{M}^{-1}\text{s}^{-1}$	Lin and Pehkonen (1997)
$\text{Hg}^+ + \text{OH} \rightarrow \text{Hg}^{2+} + \text{OH}^-$	1.0E10	$\text{M}^{-1}\text{s}^{-1}$	Lin and Pehkonen (1997)
$\text{Hg}^{2+} + \text{HO}_2 \rightarrow \text{Hg}^+ + \text{O}_2 + \text{H}^+$	1.7E4	$\text{M}^{-1}\text{s}^{-1}$	Pehkonen and Lin (1998)
$\text{Hg} + \text{HO}_2 \rightarrow \text{Hg}^{2+} + \text{O}_2 + \text{H}^-$	1.0E10	$\text{M}^{-1}\text{s}^{-1}$	^a
$\text{Hg} + \text{HOCl} \rightarrow \text{Hg}^{2+} + \text{Cl}^- + \text{OH}^-$	2.09E6	$\text{M}^{-1}\text{s}^{-1}$	Lin and Pehkonen (1998)
$\text{Hg} + \text{ClO}^- \xrightarrow{\text{H}^+} \text{Hg}^{2+} + \text{Cl}^- + \text{OH}^-$	1.99E6	$\text{M}^{-1}\text{s}^{-1}$	Lin and Pehkonen (1998)
$\text{Hg} + \text{HOBr} \rightarrow \text{Hg}^{2+} + \text{Br}^- + \text{OH}^-$	0.279	$\text{M}^{-1}\text{s}^{-1}$	Wang and Pehkonen (2004)
$\text{Hg} + \text{BrO}^- \xrightarrow{\text{H}^+} \text{Hg}^{2+} + \text{Br}^- + \text{OH}^-$	0.273	$\text{M}^{-1}\text{s}^{-1}$	Wang and Pehkonen (2004)
$\text{Hg} + \text{Br}_2 \rightarrow \text{Hg}^{2+} + 2\text{Br}^-$	0.196	$\text{M}^{-1}\text{s}^{-1}$	Wang and Pehkonen (2004)
$\text{HgSO}_3 \xrightarrow{\text{H}_2\text{O}} \text{Hg} + \text{HSO}_4^- + \text{H}^+$	0.0106	s^{-1}	van Loon et al. (2000)
$\text{Hg}(\text{OH})_2 \xrightarrow{h\nu} \text{Hg} + 2\text{OH}$	^b		Xiao et al. (1994)

^a assumed to be the same as for $\text{Hg}^+ + \text{OH}$ ^b follows a diurnal cycle with a peak of about $3\text{E}-7\text{ s}^{-1}$

Simulation of atmospheric mercury depletion events

Z.-Q. Xie et al.

Table 4. Aqueous phase equilibria.

equilibrium	K [M^{-1}]	reference
$Hg^{2+} + OH^{-} \rightleftharpoons HgOH^{+}$	4.0E10	see note*
$HgOH^{+} + OH^{-} \rightleftharpoons Hg(OH)_2$	1.58E11	see note*
$Hg^{2+} + SO_3^{2-} \rightleftharpoons HgSO_3$	2.E13	van Loon et al. (2001)
$HgSO_3 + SO_3^{2-} \rightleftharpoons Hg(SO_3)_2^{2-}$	1.E10	van Loon et al. (2001)
$Hg^{2+} + Cl^{-} \rightleftharpoons HgCl^{+}$	5.8E6	see note*
$HgCl^{+} + Cl^{-} \rightleftharpoons HgCl_2$	2.5E6	see note*
$Hg^{2+} + Br^{-} \rightleftharpoons HgBr^{+}$	1.1E9	Clever et al. (1985)
$HgBr^{+} + Br^{-} \rightleftharpoons HgBr_2$	2.5E8	Clever et al. (1985)
$HgOH^{+} + Cl^{-} \rightleftharpoons HgOHCl$	2.69E7	see note*

* value as cited by [Pan and Carmichael \(2005\)](#)

Title Page

Abstract

Introduction

Conclusions

References

Tables

Figures

⏪

⏩

◀

▶

Back

Close

Full Screen / Esc

Printer-friendly Version

Interactive Discussion



Simulation of atmospheric mercury depletion events

Z.-Q. Xie et al.

Table 5. Henry's law coefficients k_H .

reaction	k_H [M/atm]	reference
$\text{Hg} \rightleftharpoons \text{Hg}(\text{aq})$	0.13	see note ^a
$\text{HgO} \rightleftharpoons \text{HgO}(\text{aq})$	3.2E6	see note ^b
$\text{HgCl}_2 \rightleftharpoons \text{HgCl}_2(\text{aq})$	2.4E7	see note ^b
$\text{HgBr}_2 \rightleftharpoons \text{HgBr}_2(\text{aq})$	2.4E7	see note ^c
$\text{ClHgBr} \rightleftharpoons \text{ClHgBr}(\text{aq})$	2.4E7	see note ^c
$\text{BrHgOBr} \rightleftharpoons \text{BrHgOBr}(\text{aq})$	2.4E7	see note ^c
$\text{ClHgOBr} \rightleftharpoons \text{ClHgOBr}(\text{aq})$	2.4E7	see note ^c

^a value as cited by [Schroeder and Munthe \(1998\)](#)

^b value as cited by [Shon et al. \(2005\)](#)

^c assumed to be the same as for HgCl_2

Title Page

Abstract

Introduction

Conclusions

References

Tables

Figures

◀

▶

◀

▶

Back

Close

Full Screen / Esc

Printer-friendly Version

Interactive Discussion



**Simulation of
atmospheric mercury
depletion events**

Z.-Q. Xie et al.

Table 6. Initial gas-phase mixing ratios.

species	initial value	
O ₃	30	nmol/mol
Hg	0.168	pmol/mol
NO	10	pmol/mol
NO ₂	10	pmol/mol
SO ₂	100	pmol/mol
C ₂ H ₆	2000	pmol/mol
C ₂ H ₄	26	pmol/mol
C ₂ H ₂	329	pmol/mol

[Title Page](#)[Abstract](#)[Introduction](#)[Conclusions](#)[References](#)[Tables](#)[Figures](#)[I◀](#)[▶I](#)[◀](#)[▶](#)[Back](#)[Close](#)[Full Screen / Esc](#)[Printer-friendly Version](#)[Interactive Discussion](#)

Table 7. Summary of base run and sensitivity studies S1 to S20. Values that differ from the BASE run are shown in bold.

#	used in Figs.	k_{Hg+Br} [cm ³ mol ⁻¹ s ⁻¹]	k_{Hg+BrO} [cm ³ mol ⁻¹ s ⁻¹]	T [K]	CaCO ₃ precip. %	Cl chemistry on/off	Br chemistry on/off	initial SO ₂ pmol/mol
BASE	2, 3,4, 7,9	3E-13	1E-15	240	30	ON	ON	100
S1	5	—	—	240	30	ON	OFF	100
S2	5	—	—	240	30	OFF	OFF	100
S3	6	1E-14	0	240	30	ON	ON	100
S4	6	1E-13	0	240	30	ON	ON	100
S5	6,7	3E-13	0	240	30	ON	ON	100
S6	6	1E-12	0	240	30	ON	ON	100
S7	6	3.2E-12	0	240	30	ON	ON	100
S8	6,7	0	1E-15	240	30	ON	ON	100
S9	6	0	5E-15	240	30	ON	ON	100
S10	6,7	0	1E-14	240	30	ON	ON	100
S11	6	0	5E-14	240	30	ON	ON	100
S12	6	0	1E-13	240	30	ON	ON	100
S13	7	0	0	240	30	ON	ON	100
S14	7	3E-14	0	240	30	ON	ON	100
S15	8, 9,10	3E-13	1E-15	240	0	ON	ON	100
S16	9	3E-13	1E-15	240	0	ON	ON	1000
S17	9	3E-13	1E-15	240	10	ON	ON	100
S20	10	3E-13	1E-15	298	0	ON	ON	100

Simulation of atmospheric mercury depletion events

Z.-Q. Xie et al.

Title Page

Abstract

Introduction

Conclusions

References

Tables

Figures

◀

▶

◀

▶

Back

Close

Full Screen / Esc

Printer-friendly Version

Interactive Discussion



Simulation of atmospheric mercury depletion events

Z.-Q. Xie et al.

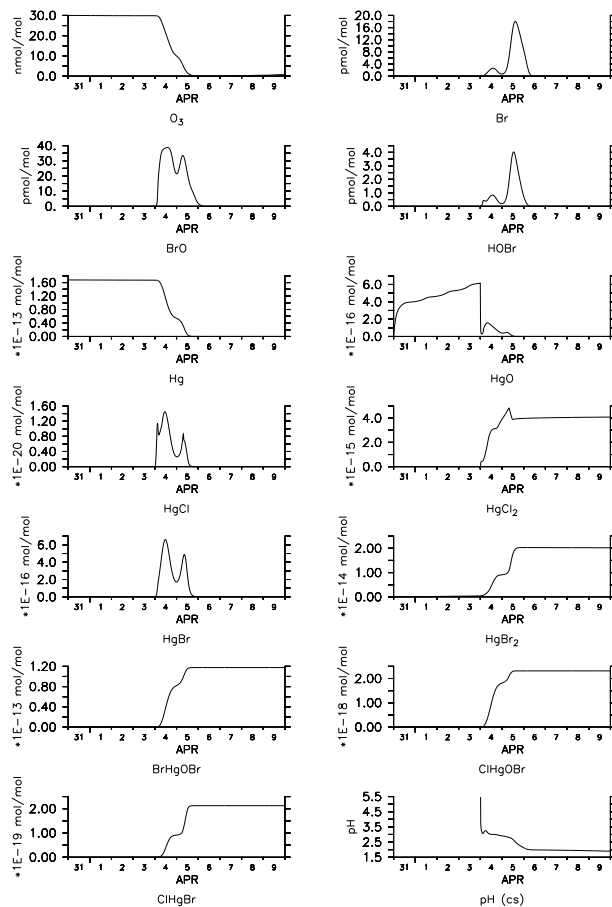


Fig. 2. Temporal evolution of model-calculated gas-phase ozone, bromine and mercury species in the BASE run. Also shown is the aerosol pH.

Title Page

Abstract

Introduction

Conclusions

References

Tables

Figures

◀

▶

◀

▶

Back

Close

Full Screen / Esc

Printer-friendly Version

Interactive Discussion



Simulation of
atmospheric mercury
depletion events

Z.-Q. Xie et al.

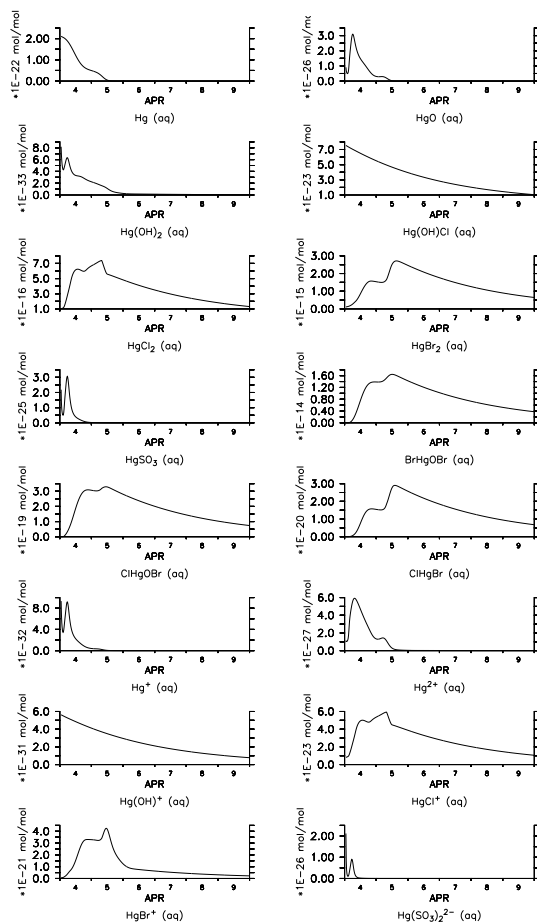


Fig. 3. Temporal evolution of model-calculated aqueous-phase mercury species in the BASE run (expressed as mixing ratios).

[Title Page](#)[Abstract](#)[Introduction](#)[Conclusions](#)[References](#)[Tables](#)[Figures](#)[⏪](#)[⏩](#)[◀](#)[▶](#)[Back](#)[Close](#)[Full Screen / Esc](#)[Printer-friendly Version](#)[Interactive Discussion](#)

Simulation of atmospheric mercury depletion events

Z.-Q. Xie et al.

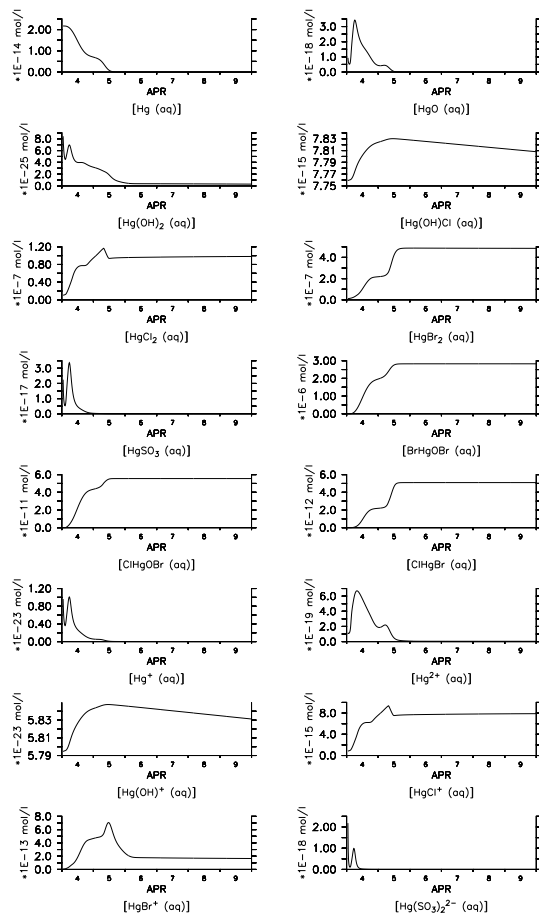


Fig. 4. Temporal evolution of model-calculated aqueous-phase mercury species (aqueous concentrations in mol/L) in the BASE run.

Title Page

Abstract

Introduction

Conclusions

References

Tables

Figures

◀

▶

◀

▶

Back

Close

Full Screen / Esc

Printer-friendly Version

Interactive Discussion



Simulation of
atmospheric mercury
depletion events

Z.-Q. Xie et al.

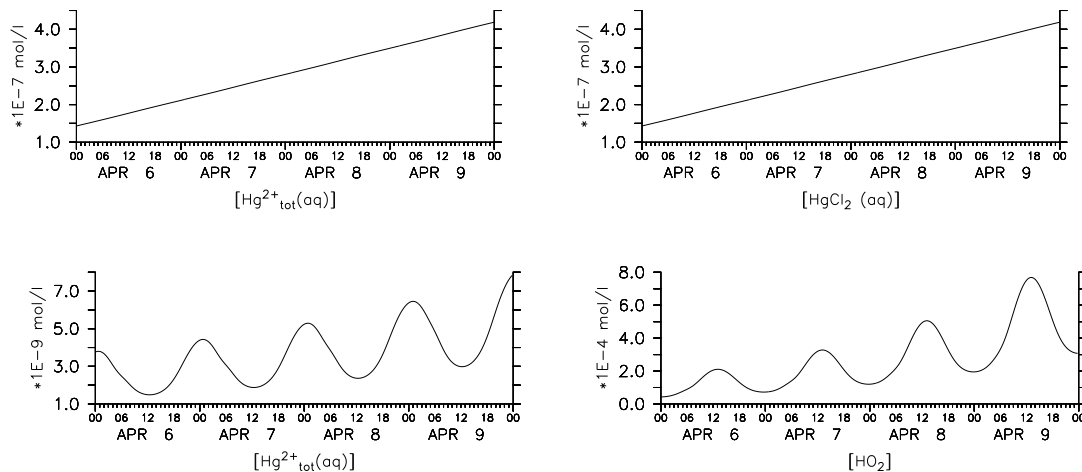


Fig. 5. Total concentration of aqueous-phase divalent mercury complexes (Hg^{2+}_{tot}). Top row: sensitivity study S1 without Br chemistry. Here, Hg^{2+}_{tot} is virtually identical to $HgCl_2$. Bottom row: sensitivity study S2 without any halogen chemistry. Here, an anticorrelation to HO_2 can be seen.

[Title Page](#)[Abstract](#)[Introduction](#)[Conclusions](#)[References](#)[Tables](#)[Figures](#)[◀](#)[▶](#)[◀](#)[▶](#)[Back](#)[Close](#)[Full Screen / Esc](#)[Printer-friendly Version](#)[Interactive Discussion](#)

Simulation of atmospheric mercury depletion events

Z.-Q. Xie et al.

——— $k(\text{Hg}+\text{Br}) = 1.0\text{E}-14$
 - - - - $k(\text{Hg}+\text{Br}) = 1.0\text{E}-13$
 - · - · $k(\text{Hg}+\text{Br}) = 3.0\text{E}-13$
 - - - - $k(\text{Hg}+\text{Br}) = 1.0\text{E}-12$
 - · - · $k(\text{Hg}+\text{Br}) = 3.2\text{E}-12$

——— $k(\text{Hg}+\text{BrO}) = 1\text{E}-15$
 - - - - $k(\text{Hg}+\text{BrO}) = 5\text{E}-15$
 - · - · $k(\text{Hg}+\text{BrO}) = 1\text{E}-14$
 - - - - $k(\text{Hg}+\text{BrO}) = 5\text{E}-14$
 - · - · $k(\text{Hg}+\text{BrO}) = 1\text{E}-13$

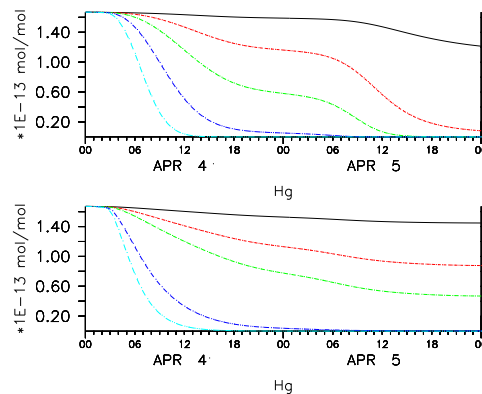


Fig. 6. Change in the paces for Hg loss with respect to the different $k_{\text{Hg}+\text{Br}}$ and $k_{\text{Hg}+\text{BrO}}$ values (unit= $\text{cm}^3 \text{mol}^{-1} \text{s}^{-1}$).

Title Page

Abstract

Introduction

Conclusions

References

Tables

Figures

◀

▶

◀

▶

Back

Close

Full Screen / Esc

Printer-friendly Version

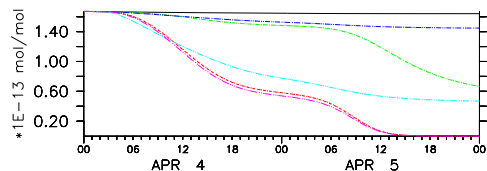
Interactive Discussion



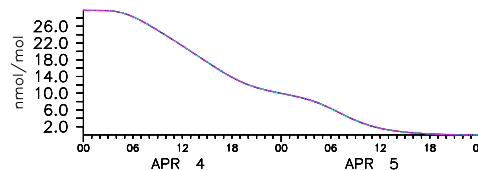
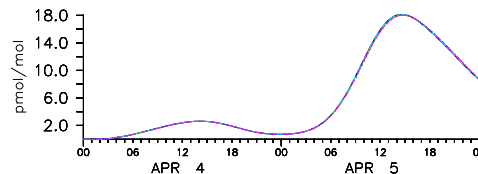
Simulation of
atmospheric mercury
depletion events

Z.-Q. Xie et al.

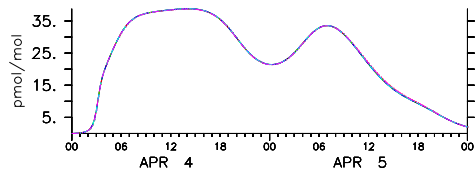
- $k(\text{Hg}+\text{Br}) = 0, k(\text{Hg}+\text{BrO}) = 0$
- - - $k(\text{Hg}+\text{Br}) = 3.0\text{E}-13, k(\text{Hg}+\text{BrO}) = 0$
- · · $k(\text{Hg}+\text{Br}) = 3.0\text{E}-14, k(\text{Hg}+\text{BrO}) = 0$
- · - $k(\text{Hg}+\text{Br}) = 0, k(\text{Hg}+\text{BrO}) = 1.0\text{E}-15$
- · · $k(\text{Hg}+\text{Br}) = 0, k(\text{Hg}+\text{BrO}) = 1.0\text{E}-14$
- · - · $k(\text{Hg}+\text{Br}) = 3.0\text{E}-13, k(\text{Hg}+\text{BrO}) = 1.0\text{E}-15$



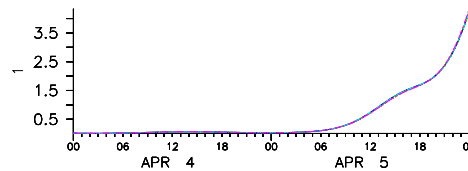
Hg

 O_3 

Br



BrO



Br/BrO

Fig. 7. The role of $\text{BrO}+\text{Hg}$ and $\text{Br}+\text{Hg}$ as a function of the Br/BrO ratio (k in $\text{cm}^3 \text{mol}^{-1} \text{s}^{-1}$).

Title Page

Abstract

Introduction

Conclusions

References

Tables

Figures

◀

▶

◀

▶

Back

Close

Full Screen / Esc

Printer-friendly Version

Interactive Discussion



Simulation of atmospheric mercury depletion events

Z.-Q. Xie et al.

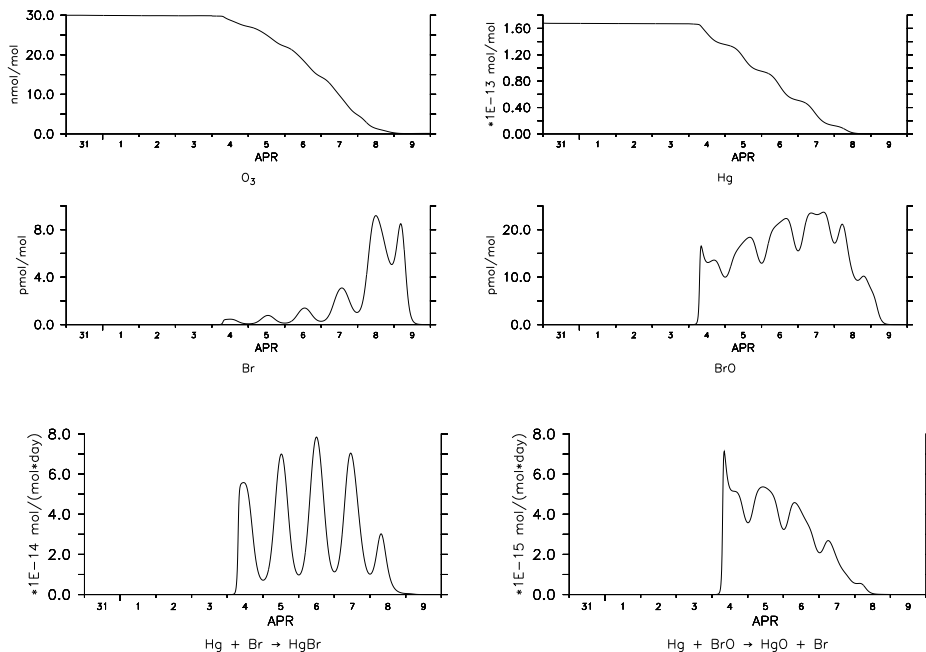


Fig. 8. Time series of O_3 , Hg, Br, and BrO during an ODE that lasts several days (sensitivity study S15, see Table 7). Also shown are the GEM destruction rates for $k_{\text{Hg}+\text{Br}}=3.0\times 10^{-13}$ and $k_{\text{Hg}+\text{BrO}}=1.0\times 10^{-15}\text{ cm}^3\text{ mol}^{-1}\text{ s}^{-1}$, respectively.

Title Page

Abstract

Introduction

Conclusions

References

Tables

Figures

◀

▶

◀

▶

Back

Close

Full Screen / Esc

Printer-friendly Version

Interactive Discussion



Simulation of
atmospheric mercury
depletion events

Z.-Q. Xie et al.

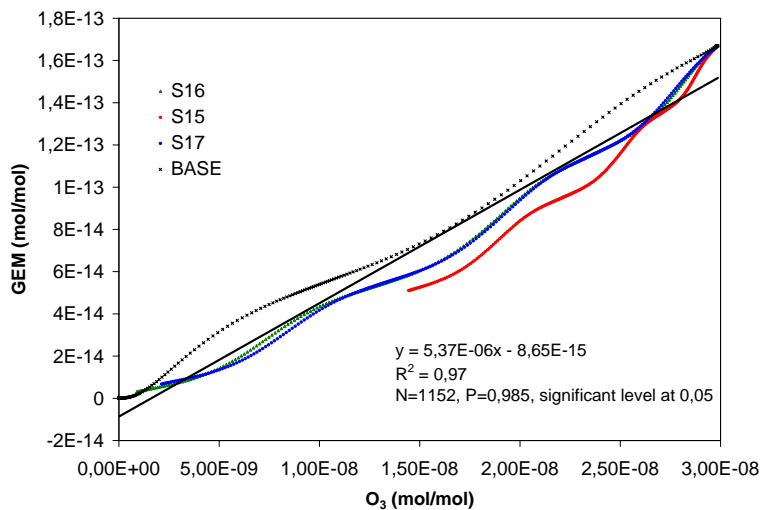


Fig. 9. Correlation between GEM and O₃ in the BASE run and in sensitivity studies S15, S16, and S17. See Table 7 for a description of the model runs.

[Title Page](#)[Abstract](#)[Introduction](#)[Conclusions](#)[References](#)[Tables](#)[Figures](#)[◀](#)[▶](#)[◀](#)[▶](#)[Back](#)[Close](#)[Full Screen / Esc](#)[Printer-friendly Version](#)[Interactive Discussion](#)

Simulation of
atmospheric mercury
depletion events

Z.-Q. Xie et al.

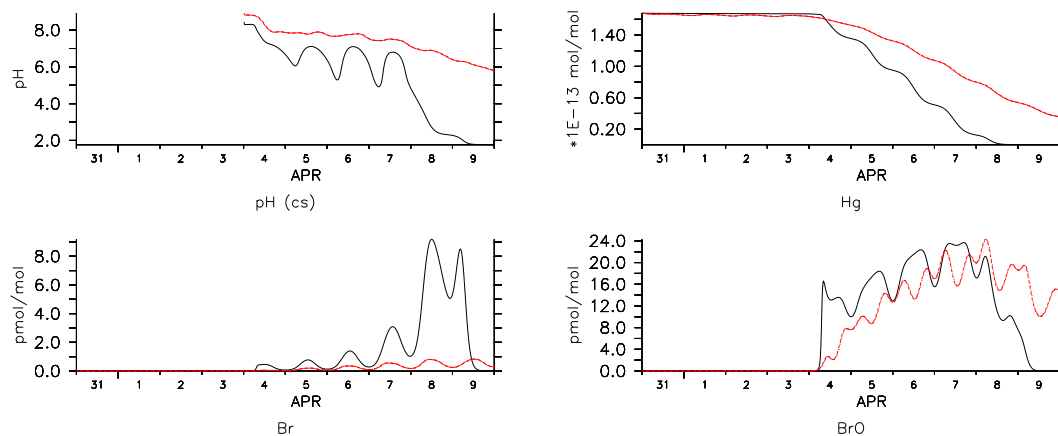


Fig. 10. The loss rate of Hg versus the different atmospheric temperature (S15=black=240 K, S20=red=298 K) in a simulation without carbonate precipitation.

[Title Page](#)[Abstract](#)[Introduction](#)[Conclusions](#)[References](#)[Tables](#)[Figures](#)[◀](#)[▶](#)[◀](#)[▶](#)[Back](#)[Close](#)[Full Screen / Esc](#)[Printer-friendly Version](#)[Interactive Discussion](#)